



**British
Geological Survey**

NATURAL ENVIRONMENT RESEARCH COUNCIL

Interactions between supercritical CO₂ and borehole cements used at the Weyburn oilfield.

Reservoir Geosciences Programme
Weyburn Monitoring and Storage Project
Commissioned Report CR/04/009

BRITISH GEOLOGICAL SURVEY

COMMISSIONED REPORT CR/04/009

Interactions between supercritical CO₂ and borehole cements used at the Weyburn oilfield.

C.A. Rochelle, J.M. Pearce, K. Bateman, D.J. Birchall and
G. Turner

Key words

CO₂, carbon dioxide, storage,
monitoring, Weyburn, borehole,
cement, wellbore, sealing,
experimental study,
geochemistry, fluid-rock
interaction.

Bibliographical reference

ROCHELLE, C.A., PEARCE, J.M.,
BATEMAN, K., BIRCHALL AND
TURNER, G. 2004. Interactions
between supercritical CO₂ and
borehole cements used at the
Weyburn oilfield. *British
Geological Survey
Commissioned Report*,
CR/04/009. 22 pp.

© NERC 2004

Keyworth, Nottingham British Geological Survey 2004

BRITISH GEOLOGICAL SURVEY

The full range of Survey publications is available from the BGS Sales Desks at Nottingham and Edinburgh; see contact details below or shop online at www.thebgs.co.uk. The London Information Office maintains a reference collection of BGS publications including maps for consultation.

The Survey publishes an annual catalogue of its maps and other publications; this catalogue is available from any of the BGS Sales Desks.

The British Geological Survey carries out the geological survey of Great Britain and Northern Ireland (the latter as an agency service for the government of Northern Ireland), and of the surrounding continental shelf, as well as its basic research projects. It also undertakes programmes of British technical aid in geology in developing countries as arranged by the Department for International Development and other agencies.

The British Geological Survey is a component body of the Natural Environment Research Council.

Keyworth, Nottingham NG12 5GG

☎ 0115-936 3241 Fax 0115-936 3488
e-mail: sales@bgs.ac.uk
www.bgs.ac.uk
Shop online at: www.thebgs.co.uk

Murchison House, West Mains Road, Edinburgh EH9 3LA

☎ 0131-667 1000 Fax 0131-668 2683
e-mail: scotsales@bgs.ac.uk

London Information Office at the Natural History Museum (Earth Galleries), Exhibition Road, South Kensington, London SW7 2DE

☎ 020-7589 4090 Fax 020-7584 8270
☎ 020-7942 5344/45 email:
bgs london@bgs.ac.uk

Forde House, Park Five Business Centre, Harrier Way, Sowton, Exeter, Devon EX2 7HU

☎ 01392-445271 Fax 01392-445371

Geological Survey of Northern Ireland, 20 College Gardens, Belfast BT9 6BS

☎ 028-9066 6595 Fax 028-9066 2835

Maclean Building, Crowmarsh Gifford, Wallingford, Oxfordshire OX10 8BB

☎ 01491-838800 Fax 01491-692345

Parent Body

Natural Environment Research Council, Polaris House, North Star Avenue, Swindon, Wiltshire SN2 1EU

☎ 01793-411500 Fax 01793-411501
www.nerc.ac.uk

Foreword

This report is the published product of a study by the British Geological Survey (BGS), and forms part of the IEA Weyburn CO₂ Monitoring and Storage Project. This project aims to monitor and predict the behaviour of injected CO₂ in the Midale reservoir at the Weyburn field in southern Saskatchewan, Canada, using methods that include time-lapse geophysics, modelling its subsurface distribution and migration, and simulating likely chemical interactions with the host rock.

This report describes fluid chemical and mineralogical changes occurring in a series of scoping experiments that have been conducted within the Hydrothermal Laboratory of the British Geological Survey. These experiments were undertaken to identify the changes that would result from the interaction of CO₂ and synthetic formation water with borehole cement. The cement samples used were of types currently used at the Weyburn field.

Acknowledgements

The authors would like to thank the European Commission (project number NNE5-2000-00096) and the UK Department of Trade and Industry (contract C/06/00296/00/00) for helping to fund this work.

The authors would like to thank their BGS colleagues whose contributions have helped make this report possible. Humphrey Wallis and Steve Upton of the R&D workshops are acknowledged for providing technical assistance and modifying pressure vessels used for the experiments. Fluid chemical analyses were carried out by Ben Charlton, Shaun Reeder, Richard Shaw and Helen Taylor.

The authors would also like to thank researchers at the University of Calgary for information on the baseline formation water chemistry of the Weyburn oil field.

Contents

Foreword.....	i
Acknowledgements.....	i
Contents.....	ii
Summary.....	v
1 Introduction	1
2 Experimental details	2
3 Details of the cement samples studied	2
3.1 Cement preparation	2
3.2 Cement analysis	3
4 Sampling and analysis.....	3
4.1 Sampling procedure	3
4.2 Preparation of experimental products	4
4.2.1 Solid products	4
4.2.2 Fluid samples	4
4.3 Analytical techniques	4
5 Results	5
5.1 Changes in size of the cement monoliths	5
5.2 Changes in weight of the cement monoliths	5
5.3 Changes in strength of cement monoliths	6
5.4 Changes in mineralogy of cement monoliths	7
5.4.1 Fill Cement (supercritical CO ₂ only, no aqueous fluid: Run 1133).....	7
5.4.2 Fill Cement (CO ₂ dissolved in synthetic Marly formation water: Run 1134) ...	8
5.4.3 Tail Cement (supercritical CO ₂ only, no aqueous fluid: Run 1135).....	8
5.4.4 Tail Cement (CO ₂ dissolved in synthetic Marly formation water: Run 1136) ..	8
5.5 Changes in composition of reacted porewaters.....	9
6 Conclusions	10
References	11
Appendix 1	22

FIGURES

Figure 1	Schematic diagram of the experimental arrangement used in this study	13
Figure 2	Schematic diagram of the Instron 3-point bend fixture	14
Figure 3	Diagrammatic representation of the output from the Instron tester during the testing of a typical cement monolith	15

PLATES

Plate 1a	Typical view of fine calcite coating external surface of a fill cement block (Run 1133, J980S101.tif)	16
Plate 1b	Tail cement matrix with a coalesced flaky texture and some fibrous outgrowths developed (Run 1135, J984S203.tif)	16
Plate 1c	Typical view of Fill cement block external surface (Run 1133, J981S203.tif)	16
Plate 1d	Oblique view of outer surface with calcite coating. (Run 1133, J980S201.tif)	16
Plate 1e	An example of clusters of radiating calcite crystals (Run 1133, J980S106.tif)	16
Plate 1f	Detailed view of larger calcite crystals on the outer surface of the cement block, which are coated in fine-grained calcite (Run 1133, J980S107.tif)	16
Plate 2a	Detailed view of larger calcite crystals on the outer surface of the cement block, which are coated in fine-grained calcite (Run 1133, J981S105.tif)	17
Plate 2b	External surface of fill cement with patchy calcite coating (Run 1134, J982S101.tif)	17
Plate 2c	Typical aggregate clusters of calcite crystals coating external surface of a tail cement block (Run 1135, J984S101.tif).	17
Plate 2d	Detailed view of calcite crystal morphologies (Run 1135, J984S102.tif)	17
Plate 2e	Tail cement matrix with clear alteration zone of denser, Ca-rich matrix, at variable depth. Note also patchy calcite precipitation on external block surfaces. (Run 1135, J984S204.tif).	17
Plate 2f	Detail of internal tail cement block with dense alteration front. (Run 1135, J985S204.tif)	17
Plate 3a	External surface of the tail cement block reacted with CO ₂ -charged synthetic marly porewater, coated in clusters of possible radiating ettringite (Run 1136, J986S101.tif)	18
Plate 3b	Curved hexagonal Ca,Al,chloride plates forming feather-like aggregates (Run 1136, J986S103.tif)	18

Plate 3c	Amorphous-looking homogenous, largely void-free, calcite and Ca,Al (\pm Cl) silicate hydrate layer coating that pre-dates other precipitates on the external surface of the tail cement block reacted with CO ₂ -charged synthetic marly porewater. (Run 1136, J986S104.tif)	18
Plate 3d	Irregular radiating ettringite aggregates post-dating amorphous-looking Ca sulphate, chloride coating	18

TABLES

Table 1	Listing of the CO ₂ experiments conducted during this study, together with details of the sizes of the monoliths used	19
Table 2	Listing of all the experiments conducted during this study, together with details of the weights of the monoliths used	20
Table 3	Listing of all the experiments conducted during this study, together with details of the strengths of the monoliths used	21

Summary

This report describes work undertaken at the British Geological Survey (BGS) that forms part of the IEA Weyburn CO₂ Monitoring and Storage Project. This project aims to monitor and predict the behaviour of injected CO₂ into the Midale reservoir at the Weyburn oil field in southern Saskatchewan, Canada, using methods that include time-lapse geophysics, modelling its subsurface distribution and migration, and simulating likely chemical interactions with the host rock. This report describes fluid chemical and mineralogical changes occurring in a series of experiments that have been conducted within the Hydrothermal Laboratory of the British Geological Survey. These experiments were undertaken to identify the changes that would result from the interaction of CO₂ and synthetic formation water with borehole cement.

The scoping experiments summarised in this report used samples of borehole cement of types currently used at the Weyburn field ('fill' and 'tail' cements), together with synthetic porewaters based upon actual measured well fluid compositions. The pressures and temperatures used within the experiments were representative of actual *in-situ* conditions at Weyburn (60°C, 150 bar [15 MPa]), conditions that will exist even after oil production and CO₂ injection have ceased. The experiments were pressurised with either CO₂ or N₂, and had durations of two weeks. Although this timescale was relatively short, there was enough reaction to provide some insights into the reactions of borehole cements with CO₂.

No significant changes in the size of the cement monoliths were found after exposure to CO₂. However, sample density increased significantly. The fill cement underwent a greater weight increase (approximately 9-12%) compared to the tail cement (approximately 1-4%). However, for both fill and tail cement, weight gain was greater with supercritical CO₂ (11% and 4% respectively) compared to dissolved CO₂ (10% and 1% respectively).

Simple flexure tests showed no significant changes in the tensile strength of the cements after exposure to CO₂. However, the fill cement was about twice as strong as the tail cement (both before and after exposure to CO₂). There were some tentative indications from the fill cement experiments that leaching by aqueous fluids may have decreased cement strength a little.

Both tail and fill cements reacted with the CO₂, developing calcite coatings up to 40 µm thick on most external surfaces. This 'carbonation' reaction also penetrated into the cement blocks to varying depths up to around 3.5 mm from the block surface (depending on experimental duration and local permeability variations). The carbonation reaction produced a probable calcite-rich front with significantly reduced porosity that varied up to 50-100 µm in thickness. In contrast to the fill cement, the tail cement reacted extensively with the CO₂-rich synthetic 'Marly porewater' to produce a series of precipitates from probable calcite and CSH gel, to ettringite and Ca-sulphate, chloride. However, more detailed studies are needed to identify definitively and quantify the reaction products developed in these experiments.

Changes in fluid chemistry reflected control by cement minerals in both the lower pH CO₂ experiments and the hyperalkaline CO₂-free experiments. Large decreases in Mg in the CO₂-free experiments suggest brucite precipitation, compared to possible brucite dissolution and increases in Mg in the CO₂ experiments. Data for Si show similar trends, and suggest control by CSH phases. Very high bicarbonate concentrations were found in the CO₂ experiments.

Overall, this study found no evidence for significant deleterious reactions – at least in the short term. However, our relatively simple approach will have not replicated all of the complex spatial and temporal variations around a borehole. Much work remains to be done to

develop a comprehensive understanding of the interactions of stored CO₂ with borehole cement, and especially those operating over the longer term.

1 Introduction

The IEA Weyburn CO₂ Monitoring and Storage Project is a collaborative investigation, involving geoscientists from North America and Europe (Moberg, 2001). It is studying the geological sequestration of CO₂ during an enhanced oil recovery (EOR) operation at the Weyburn oil field, Canada. By the end of the EOR phase, it is expected that approximately 20 million tonnes of anthropogenic CO₂ will have been stored deep underground. Climate-warming greenhouse gas emissions will have been reduced in an efficient and cost-effective manner.

The Weyburn oilfield is located in southern Saskatchewan, Canada. It was discovered in 1954 and is owned and operated by the EnCana Corporation (formerly PanCanadian). Oil is recovered from the uppermost Midale Beds of the Charles Formation, a succession of upwards shoaling, shallow marine carbonate-evaporite sediments of Mississippian age. The Midale Vuggy unit contained most of the oil produced from the Weyburn field to date, and is now nearing exhaustion. This unit represents open marine conditions and is overlain by the shallow water dolomitic mudstones of the Midale Marly Beds. Post-diagenetic dolomitisation of this later unit created good reservoir properties, which are now the target for the miscible CO₂ flood. The Midale Marly Beds are overlain by the Midale Evaporite unit, which acts as a local seal (caprock) preventing oil (and CO₂) migration.

During underground CO₂ storage operations in deep reservoirs, the CO₂ can be trapped in three main ways (with descriptors from Bachu *et al.*, 1994):

- as 'free' CO₂, most likely as a supercritical phase (physical trapping)
- dissolved in formation water (hydrodynamic trapping)
- precipitated in carbonate phases such as calcite (mineral trapping)

For CO₂-EOR operations, the CO₂ can also be trapped as a dissolved phase within residual oil remaining within the formation after the end of production.

It is important to prevent migration of stored CO₂ (as either a free phase or a dissolved phase - as outlined above) into overlying formations or even back to the atmosphere. As a consequence, it is vital that the seals containing the CO₂ remain as effective as possible. This includes the man-made 'engineered' seals around boreholes (steel and cement) as well as the natural caprock seal. The experimental scoping study summarised here, focussed on the reactions between CO₂, porewaters and borehole cement. Although borehole cement represents only part of the borehole infrastructure (the other being the steel well liner), it is especially important as it forms the bond/seal between the steel liner and the rock.

The scoping experiments summarised in this report used samples of borehole cement of types currently used at the Weyburn field, together with synthetic porewaters based upon measured well fluid compositions. The pressures and temperatures used within the experiments were representative of *in-situ* conditions at Weyburn (60°C, 150 bar [15 MPa]), conditions that will exist even after oil production and CO₂ injection have ceased.

This work built upon experience gained in earlier experimental studies (e.g. Czernichowski-Lauriol *et al.*, 1996; Gunter *et al.*, 1993; Rochelle *et al.*, 2002a). The procedures used are based upon those given in Rochelle *et al.* (2002b), which were used successfully in subsequent studies of Midale rock material (Rochelle *et al.*, 2002c; Rochelle *et al.*, 2003a,b,c, Bateman *et al.*, 2004).

2 Experimental details

In order to obtain a better understanding of cement-water-CO₂ interactions, several relatively short-term ‘batch’ experiments have been performed. This type of equipment is relatively simple and generally free from day-to-day maintenance, and has been used successfully in previous studies of CO₂-water-rock reaction (e.g. Czernichowski-Lauriol *et al.*, 1996; Rochelle *et al.*, 2002a).

The batch reactor vessels were of relatively small volume (<200 ml), but they were large enough to accommodate two cement ‘monoliths’ and a dip tube for fluid sampling (Figure 1). The monoliths (of approximately 1x1x5 cm) were oriented horizontally within the reactor to ensure they could be covered with synthetic formation water. Fluid:cement ratios (by weight) were typically in the order of 4:1. The fluid used in the experiments was based on analyses of formation waters at Weyburn from the University of Calgary (Shevallier, pers. comm.), and was the same synthetic formation water as used in the Midale Marly experiments (Rochelle *et al.* 2003a).

Three types of experiments were conducted during this study in the batch reactor vessels:

- 1) Cement only, and pressurised with CO₂. These ‘reactive’ experiments provided information on the chemical and mineralogical changes that might occur during the direct interaction of dry supercritical CO₂ with borehole cements at the Weyburn oil field. These experiments should have produced greatest reaction as they had the highest concentrations of CO₂ in direct contact with the cement monoliths.
- 2) Cement, synthetic Midale Marly Formation, and pressurised with CO₂. These ‘reactive’ experiments provided information on the chemical and mineralogical changes that might occur during the interaction of dissolved CO₂ with borehole cements at the Weyburn oil field.
- 3) Cement, synthetic Midale Marly Formation, and pressurised with N₂. These provided baseline ‘non-reacting’ cases, which could then be compared to the ‘reactive’ CO₂ experiments.

Details of the experiments are presented in Appendix 1 and Tables 1-3.

3 Details of the cement samples studied

The two cement samples studied represented the types of borehole cement used currently at Weyburn. They were received from BJ Services Company Canada, as pre-prepared powders that only needed water adding to them. The cement samples were basically Portland cement with additives. The cement descriptors ‘tail cement’ and ‘fill cement’ were as used by BJ Services:

Fill cement: “1:1:2G + 0.5% CD-31”

Tail cement: “Thix Mix G + 0.4% FL-77 + 2.0% CaCl₂”

3.1 CEMENT PREPARATION

Both of the cement types were prepared in a similar way according to the instructions from BJ Services Company Canada (Fraser, pers. comm.):

Fill cement: “1:1:2G + 0.5% CD-31”

328.9 g of this dry mix was added to 177.5 ml of water, and the resulting slurry well mixed with a PEEK 2-loop ‘whisk’ at approximately 6300 rpm for 5 minutes.

Tail cement: “Thix Mix G + 0.4% FL-77 + 2.0% CaCl₂”

337.8 g of this dry mix was added to 194.5 ml of water, and the resulting slurry well mixed with a PEEK 2-loop 'whisk' at approximately 6300 rpm for 5 minutes.

Both of the above cement samples were prepared in such a way as to try to reproduce the conditions that actual borehole cement might undergo during emplacement. This included making up under aerobic conditions, setting under *in-situ* pressures but at reduced temperatures, and finally curing for 28 days under both *in-situ* pressure and temperature.

Once mixed, the cement slurry was placed into a 50 mm internal diameter high density polyethylene (HDPE) tube which was well sealed with HDPE bungs at each end. No gas (air) remained once this was assembled. The plastic slurry holder was then sealed into a plastic bag full of Ar, and the whole assembly placed into a steel pressure vessel and pressurised with 15 MPa (150 bar) of Ar. After 24-48 hours the pressure vessel was warmed to 60°C whilst still at pressure, and this temperature maintained for 28 days. After this the cylinders of now set and cured cement were extracted and stored under Ar and over water. An Ar atmosphere was used to minimise the potential for carbonation reactions with atmospheric CO₂ prior to the experiments.

When set, both of the cement types were grey, uniform, fine-grained solids. In order to produce 1x1x5 cm monoliths, they were cut by hand on a diamond-edged rotary saw. No special sample holders were used during this cutting procedure, and this meant that a little non-uniformity in sample size was inevitable. However, given the scoping study nature of this investigation, this was felt appropriate. By and large, all cuts were made within about 10% of their desired position (see Table 1 for details of exact sample dimensions).

3.2 CEMENT ANALYSIS

The fill cement structure comprised Na,K,Mg±Ca Al-Silicate bubbles entrained within a matrix of similar composition (Ca(±Na?,Fe,SO₄)MgAl-silicate hydrate±S,Fe) and extensive calcite (Plate 1a). This matrix occasionally developed a welded flaky habit. Generally rare, more fibrous cement matrix (CSH?) developed in the voids around the spheres.

The tail cement lacks the spheres seen in the fill cement. Energy dispersive X-ray analysis (EDXA) indicated that the matrix was calcite plus calcium silicate hydrate gel (±Mg,Al,SO₄,Cl) and had a coalesced flaky texture with some fibrous outgrowths developed (Plate 1b). It contained short calcite laths, typically 1-2 µm long.

4 Sampling and analysis

Samples from both CO₂-pressurised and N₂-pressurised experiments are treated in the same way.

4.1 SAMPLING PROCEDURE

At the end of the experiments a single, large aqueous fluid sample was extracted that (ideally) contained all of the aqueous fluid within the reactor. This sample was taken by degassing it straight into a sterile syringe – several aliquots were taken to ensure near complete removal of the aqueous phase. The syringe was modified to allow excess gas to escape, but to retain the aqueous sample. The aqueous samples were then treated as detailed in Section 4.2.2. As much aqueous fluid as possible was removed from the reactor. This was done to minimise the potential for carbonate mineral precipitation as a result of the solution degassing (basically this would be an artefact of sampling).

Previous experience indicated that degassing of reacted solutions could result in carbonate mineral precipitation. However, usually this only occurred after a few hours. Consequently, for the aqueous samples that are taken and preserved in a matter of a few tens of minutes, such precipitation is not thought to represent a significant problem.

Depressurisation of the (now only damp) cement monoliths within the reactor typically took approximately 10 minutes.

4.2 PREPARATION OF EXPERIMENTAL PRODUCTS

4.2.1 Solid products

On opening a batch pressure vessel, its PTFE liner containing the (hopefully only slightly damp) samples of reacted cement was removed. After this, the samples were washed in a very little de-ionised water (to reduce the potential for halite formation on drying), patted dry with a tissue, and stored in an Ar atmosphere over water.

4.2.2 Fluid samples

After sampling into a polythene syringe, each of the reacted fluids was split into two main sub-samples:

- 1) The first sub-sample (approximately 1 ml) was taken for immediate analysis of pH.
- 2) The second sub-sample was filtered using a 0.2 μm 'Anotop'® nylon syringe filter:
 - i) A volume (in the order of 12 ml) of this sub-sample was placed into a polystyrene tube and acidified with 1% (i.e. in the order of 0.12 ml) of concentrated 'ARISTAR'® nitric acid. This was analysed subsequently for major and trace cations by inductively coupled plasma - optical emission spectroscopy (ICP-OES).
 - ii) A further aliquot (in the order of 2 ml) was taken and placed into a polyethylene tube and analysed subsequently for anions by ion chromatography (IC). This sample was typically diluted to 50% with de-ionised water, in order to minimise potential carbonate mineral precipitation.
 - iii) A final aliquot (in the order of 2 ml) was taken and placed in a polystyrene tube for immediate analysis of bicarbonate/carbonate.

Samples for ICP-OES and IC were stored in a fridge (at about 5°C) prior to analysis in batches.

4.3 ANALYTICAL TECHNIQUES

Standard methods of analysis of solid and liquid samples were employed in this study, and are comparable to those detailed in *Rochelle et al.* (2002b). In brief, appropriate fluid samples were taken for chemical analysis of major (\pm some minor) cations using inductively coupled plasma - optical emission spectroscopy (ICP-OES), and for all major (\pm some minor) anions using ion chromatography (IC). pH measurements were made on cooled and depressurised samples using an Orion® 900A pH meter. This was calibrated using three Whatman® NBS traceable buffers chosen from pH 4, 7, 10 and 13.

The cement blocks were dried under argon to minimise further reaction. Internal and external surfaces were examined by scanning electron microscopy (SEM) in a Leo 435VP variable pressure instrument fitted with an Oxford Instruments Isis energy-dispersive X-ray microanalysis system that enabled semi-quantitative chemical analyses to aid mineral identification. A 20kV accelerating voltage was routinely used. It should be noted that although semi-quantitative chemistries were obtained wherever possible, the fine-grained

nature of the cements and reaction products, plus the variable chemistries of many cement phases, means that mineral identifications should be considered tentative.

5 Results

The samples of borehole cement arrived relatively late in the experimental programme. As a consequence, the experiments were run for only 2 weeks and complete reaction to steady-state conditions was not achieved. However, enough reaction occurred to provide an indication of the processes occurring.

5.1 CHANGES IN SIZE OF THE CEMENT MONOLITHS

Observations from the construction industry have identified shrinkage of cement during carbonation (e.g. Lea, 1970; Mehta, 1994; DePuy, 1994). This can lead to degradation of the cement through a process of cracking, followed by ingress of air and water, and eventual corrosion of reinforcing steel. This process is primarily a consequence of dehydration during carbonation. Although borehole cement deep underground is much less likely to undergo dehydration, some simple measurements were taken to ascertain whether a measurable change in cement monolith size would occur during the 2 weeks duration of the experiments.

The dimensions of each cement monolith were measured with an electronic engineers scale, which was accurate to 10 μm . Three measurements of height and width were made down the monoliths (at each end and in the middle), together with a single measurement of monolith length. Each monolith was marked with an individual gold wire tag at one end so that comparable measurements could be made before and after reaction. The results obtained for the CO_2 experiments are given in Table 1.

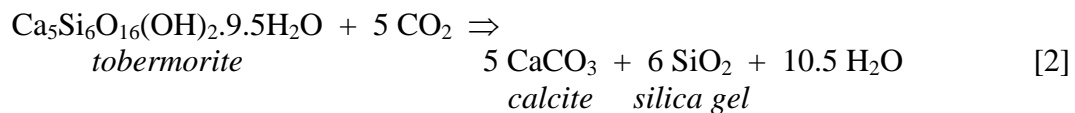
The results show that there was negligible change in the dimensions of the monoliths during these (albeit relatively short) experiments. That no evidence for cement shrinkage was observed is a positive result in terms of CO_2 containment.

5.2 CHANGES IN WEIGHT OF THE CEMENT MONOLITHS

During cement carbonation, CO_2 is taken up by the cement and precipitated as CaCO_3 . The reaction could proceed via:



though a whole variety of reactions involving carbonation of calcium silicate hydrate (CSH) phases could also be involved:



For reaction [1], if water were not lost from the cement this would equate to a weight gain of about 59%. However, if water loss is assumed, then the weight gain is only about 35%. Each cement monolith was therefore carefully weighed before and after reaction to assess the degree of carbonation. Any excess water on the outer surfaces of the monoliths was removed with a tissue prior to weighing, but the monoliths were not dried any further. It should be noted that the monoliths may have had some pores not totally filled by water, and so variable saturation was possible. The weight results obtained are given in Table 2.

The results show that carbonation results in an increase in weight for both the fill cement and the tail cement. However, the fill cement undergoes a greater weight increase (approximately 9-12%) compared to the tail cement (approximately 1-4%). As a consequence, it appears that the fill cement has carbonated much faster than the tail cement. Weight increases on carbonation have been observed in other studies (e.g. Van Ginneken *et al.*, 2004).

It is also apparent that the form of the CO₂ has an impact on degree of carbonation. For both cement types, more weight gain is found in the experiments with just supercritical CO₂ (11% and 4%) compared to the equivalent experiments where the CO₂ was in dissolved form (10% and 1%). This could result from there being much more CO₂ available to react in the supercritical phase compared to when it is dissolved in water. However, it could also be a consequence of easier access of CO₂ into the cement. Reactions [1] and [2] generate water, and as this fills pores it will hinder the access of CO₂ (Reardon *et al.*, 1989).

In terms of the overall degree of carbonation, it is hard to make a precise determination of exactly how carbonated the samples were during the 2 weeks of reaction. In part this is because of not knowing which specific carbonation reactions were occurring (e.g. those involving Ca(OH)₂ or CSH phases etc). However, we also did not measure changes in water content of the experiments. The difficulties with this latter point were particularly evident at the end of the ‘supercritical CO₂ only’ experiments, where droplets of water were seen on the surfaces of the monoliths, even though their surfaces were relatively dry prior to reaction. Although this ‘excess water’ may have been a result of reaction, it could equally have been due to expansion of free CO₂ inside the monolith pushing out pore water and leaving the reacted monolith relatively undersaturated. What is clear however, is that loss of water would lead to underestimations of the degree of carbonation. The weight change results therefore, represent at least *minimum* degrees of carbonation.

Given that the monoliths remained the same size as they were prior to reaction and increased in weight, then they must have increased in density. The scope of this study did not involve a detailed analysis of porosity changes at the monolith surfaces. However, initial mineralogical observations have identified low porosity/permeability carbonated layers (see Section 5.4). It is possible that such layers could act to ‘armour’ cement against further reaction (or at least reduce it).

5.3 CHANGES IN STRENGTH OF CEMENT MONOLITHS

Strength testing was done by measuring the force required to snap a 5x1x1 cm monolith in half. This was done using an Instron strength tester (Model 1011) fitted with a 2810 Series 3-point bend fixture. The monolith sample was mounted on top of, and straddled, two supports some 4 cm apart. A force was then applied to the centre of the monolith from above via a moveable anvil (Figure 2), which moved downwards at a constant rate of 1 mm per minute. All contacts with the monoliths were via smooth, curved surfaces. Above the anvil was a transducer, which measured the force applied to the monolith. This was calibrated against a known weight of 5 kg prior to the tests. The effect of the tests can be demonstrated in Figure 3. Initially, there is a phase when the anvil is moving down onto the monolith. Once contact with the monolith is made, the force applied increases steadily and approximately linearly over time. Finally, the monolith cracks in half and the force applied to the sample drops to zero. The Instron tester recorded and displayed the maximum force applied (in kg) at the point of monolith failure (Table 3). The output of the transducer (Voltage signal) was also logged directly by an external Picolog logger every 50 ms (Table 3).

Several points should be borne in mind when considering the results:

- 1) These tests were relatively simple, and only designed to pick up fairly large changes in cement strength. The results should therefore not be overly interpreted.
- 2) The monoliths were not all exactly the same shape. This will have meant that some monoliths were bigger and stronger than others, and a $\pm 10\text{-}15\%$ variability in the results may be a reasonable estimate of uncertainty.
- 3) Any mishandling of the sample during preparation may have induced weak points or microfractures. These artefacts may make an individual sample weaker than it would otherwise be. Although duplicate samples were run to try to identify such artefacts, they only provide an indication of uncertainty. Constraints of time and reaction vessel size prevented the ageing and reaction of a more statistically-meaningful number of samples.

Several conclusions can be determined from the results:

- 1) The fill cement is about twice as strong as the tail cement (both before and after exposure to CO_2).
- 2) For the fill cement, there appears to be no real difference between the strength of the unreacted material and the samples exposed to either supercritical CO_2 or dissolved CO_2 .
- 3) For the fill cement, the monoliths exposed to synthetic formation water under N_2 pressure seem to be somewhat weaker than the starting material or the samples exposed to CO_2 .
- 4) Data availability for the tail cement is not as good as for the fill cement. However, there are tentative indications that exposure to supercritical CO_2 does not markedly reduce cement strength. Variability in, and coverage of, the other results make it unclear as to the relative importance of carbonation versus leaching on tail cement strength.

Overall therefore, although this investigation of cement strength was relatively simple, many of the monolith samples appeared to retain their strength after (limited amounts of) carbonation. This is in contradiction to some previous studies, which identified greatly reduced cement strength on exposure to elevated pressures of CO_2 (e.g. Robins and Milodowski, 1982). However, the results of this study have also not demonstrated improvements in cement strength as seen in some other studies (e.g. DePuy, 1994; Gibbs, 1996; Lea, 1970). The indications that these borehole cement samples may indeed retain much of their original strength is a generally positive result in terms of CO_2 containment, though much work remains to be done in the area of CO_2 -cement interactions.

5.4 CHANGES IN MINERALOGY OF CEMENT MONOLITHS

Initial observations showed that the CO_2 produced carbonation of the outer parts of the monolith samples (20% or so), which was associated with an apparent reduction in porosity of the outer parts of the monoliths. Time constraints meant that only some of the monoliths reacted with CO_2 were studied, and not those from N_2 -pressurised experiments. More extensive work would be needed to provide a full and detailed characterisation of the complex reaction products formed in the cement experiments.

5.4.1 Fill Cement (supercritical CO_2 only, no aqueous fluid: Run 1133)

The outer surface of the block was completely covered in a coating of interlocking, fine-grained, subhedral to euhedral, elongate calcite (possible aragonite) crystals with irregular terminations. Individual crystals are typically around $5\text{-}10\text{ }\mu\text{m}$ long with submicron intercrystalline porosity (Plate 1c) and form a crust approximately $40\text{ }\mu\text{m}$ thick (Plate 1d).

Developing from this coating were larger radiating clusters of calcite that were approximately 100 μm across. Individual crystals were around 20 μm long and had three-fold symmetry (Plate 1e). These larger crystals were coated in more fine-grained calcite (Plates 1f and 2a). Calcite also occasionally formed hexagonal platelets. Rare gypsum also developed as coarse 100 μm subhedral to euhedral crystals. These are thought to post-date the calcite since they are not covered by fine-grained calcite.

There does not appear to be any textural or mineralogical differences between the outer edge and the centre of the cement block. The internal cement structure comprises Na,K,Mg \pm Ca Al-Silicate bubbles entrained within a matrix of similar composition (\pm S,Fe) but with extensive calcite as well.

5.4.2 Fill Cement (CO₂ dissolved in synthetic Marly formation water: Run 1134)

In contrast to Run 1133, the external surfaces of the cement blocks reacted with CO₂ in synthetic Marly formation water were more variably coated with relatively poorly developed calcite (Plate 2b), plus some halite, a artefactual product of sample drying. The aggregate clusters of subhedral to euhedral crystals developed in Run 1133 were not developed in Run 1134. Some external surfaces, however, were similar to those in Run 1133 with a more extensive calcite coating. Rare, poorly developed, subhedral coarser calcite crystals were occasionally found.

5.4.3 Tail Cement (supercritical CO₂ only, no aqueous fluid: Run 1135)

The external surface of this tail cement block, was different to the fill cements described above. Calcite developed in aggregates of radiating clusters, often themselves clustered together to form millimetre-scale patches (Plate 2c). However, unlike the previous samples where the crystals, though generally subhedral, had a poorly-formed ragged morphology, here the crystals were elongate euhedral rods of hexagonal cross-section with diameters typically between 5 and 10 μm (Figure 2d). In some areas these crystals developed bladed morphologies. Underlying these aggregate clusters was a massive calcite coating formed from an interlocking mosaic of anhedral micron-scale crystallites. This block was broken by hairline cracks probably developed during either experimental depressurisation or flexure tests.

An irregular zone of alteration, clearly visible with the naked eye, penetrated from the outer surface into the block. In the SEM the irregular boundary between this region of alteration and the cement matrix was marked by zone 50-120 μm across with a denser, less porous texture (Plate 2e). This zone developed up to a depth of 3.5 mm. EDXA indicates that this zone was dominated by Ca, but appears to have more Si and less Al than the internal cement matrix. The matrices on both sides of this boundary had very similar compositions to this zone but with possible more SO₄ and Cl and are texturally more porous and less dense than the boundary (Plate 2f).

5.4.4 Tail Cement (CO₂ dissolved in synthetic Marly formation water: Run 1136)

Aggregate radiating clusters of acicular needles were formed on the external surfaces of the cement blocks, which EDXA indicated to be of Ca,Al sulphate (ettringite?) chemistry (Plate 3a). Calcite formed a patchy, coarse, anhedral coating across the surface. Ca,Al,chloride crystals formed curved hexagonal plates in feather-like aggregates that may pre-date the ettringite (Plate 3b). Underlying this was an amorphous-looking homogenous, largely void-free, calcite and Ca,Al (\pm Cl) silicate hydrate coating which had dried to form a network of shrinkage cracks (Plates 3c and 3d).

5.5 CHANGES IN COMPOSITION OF REACTED POREWATERS

The experiments were run for only 2 weeks, and it is unlikely that steady-state solute concentrations were achieved on this timescale. As a consequence, only limited conclusions can be drawn about the changes in chemistry of the reacted waters. The available data are given in Appendix 1. A few comments on the more significant changes are as follows:

- 1) *Depressurised pH.* The pH in the experiments pressurised with N₂ rose to about 12 as the synthetic formation water equilibrated with the minerals in the cement samples. The presence of a constant supply of CO₂ appears to have overcome this pH increase and maintained it at about pH 7.
- 2) *Bicarbonate and carbonate.* The presence of both cement and CO₂ resulted in significant concentrations of dissolved bicarbonate as the (acidic) CO₂ was neutralised by the (alkaline) cement. Dissolved C concentrations were lower in the N₂-pressurised experiments, and dominated by carbonate due to the higher pH conditions.
- 3) *Magnesium.* The CO₂ pressure increased Mg concentrations by some 50-300%, presumably through the breakdown of phases such as brucite (Mg[OH₂]) or silicate hydrate in the cement. In the absence of CO₂ however, reaction with the cement caused the pH to rise to the point where a secondary Mg phase was stable (e.g. brucite). This caused all of the Mg originally in the synthetic formation water to precipitate as this phase.
- 4) *Silica.* Reaction between CO₂, synthetic formation water and both samples of cement, resulted in a 3-4 fold increase in dissolved Si concentrations. The source of the Si could be from calcium silicate hydrate (CSH) phases in the cement. It is not possible to say which phase was controlling dissolved Si concentrations, but it might be amorphous silica as this phase is commonly seen as a secondary phase after cement carbonation (e.g. Reardon *et al.*, 1989, and see equation [2]), and this could be controlling dissolved Si concentrations. The (alkaline) N₂-pressurised experiments have Si concentrations that are lower than in the synthetic formation water. This suggests that Si is being precipitated as a secondary phase. Previous studies (Savage *et al.*, 1992) have identified that hyperalkaline Ca-rich solutions will be Si-poor due to rapid equilibration with CSH phases, and a similar process would appear to be happening in these experiments.
- 5) *Aluminium.* All solutions have Al concentrations that are either very low or below detection limits. Although Al should be more soluble in alkaline solutions (such as in the N₂-pressurised experiments), it is readily taken up in CSH phases - phases that appear to have been precipitating in the experiments. The absence of measurable concentrations of dissolved Al in the CO₂-pressurised experiments would concur with a model of secondary mineral precipitation (e.g. such as dawsonite or Al-rich CSH phases).

The types of changes described above, and their dependence on pH, are generally in accord with known cement mineral behaviour. No evidence was found to suggest that current models of the behaviour of cement in the geosphere would be unsuitable for investigations of cement-CO₂ interactions. However, much work remains to be done in this complex area of CO₂-cement interactions.

6 Conclusions

A series of laboratory experiments were undertaken to identify geochemical changes resulting from the reaction of CO₂ with borehole cement samples typical of those used at the Weyburn oilfield. The pressures and temperatures used within the experiments represented *in-situ* conditions at Weyburn (60°C, 150 bar [15 MPa]), conditions that will exist even after oil production and CO₂ injection have ceased. The experiments were of relatively short duration (only 14 days), and so only limited reaction was observed. However, enough reaction occurred to provide some insights into the reactions of borehole cements with CO₂.

Two samples (termed ‘fill cement’ and ‘tail cement’) of cement were prepared and cured under *in-situ* conditions for 28 days. After the curing stage, they were then cut into 1x1x5 cm monoliths for reaction in the experiments. These involved reaction with either; just supercritical CO₂, maximum amounts of dissolved CO₂ (i.e. in equilibrium with 150 bar [15 MPa] of supercritical CO₂ at 60°C), or N₂-pressurised synthetic formation water (‘non-reacting’ base case for comparison).

No significant changes in the size of the cement monoliths were found after (relatively short term) exposure to CO₂. Although this does not preclude the possibility that carbonation shrinkage will occur, it does provide some evidence that this process might not be an important issue over shorter timescales. In terms of CO₂ containment issues, these results are generally positive.

The cement monoliths gained weight on exposure to CO₂. The fill cement underwent a greater weight increase (approximately 9-12%) compared to the tail cement (approximately 1-4%). However, for both fill and tail cement, more weight gain occurred with just supercritical CO₂ (11% and 4% respectively) compared to dissolved CO₂ (10% and 1% respectively). This weight gain was associated with an increase in density, and initial mineralogical observations have identified that this is associated with low porosity/permeability carbonated layers. It is possible that such layers could act to ‘armour’ cement against further reaction (or at least reduce it). In terms of CO₂ containment issues, these results appear to be generally positive.

A few relatively simple flexure tests were carried out to assess cement strength changes upon carbonation. Although data are few and results are preliminary, no significant changes in the tensile strength of the cement monoliths were found after (relatively short term) exposure to CO₂. What was apparent however, was that the fill cement was about twice as strong as the tail cement (both before and after exposure to CO₂). There were some indications from the fill cement experiments that leaching by aqueous fluids may have decreased cement strength a little, though these results are tentative. Overall however, these initial indications show that borehole cement may indeed retain much of its original strength upon exposure to CO₂. This is a generally positive result in terms of CO₂ containment issues, though much work remains to be done in this area.

Both tail and fill cements reacted with the CO₂, developing calcite coatings up to 40 µm thick on most external surfaces. This ‘carbonation’ reaction also penetrated into the cement blocks to varying depths, depending on experimental duration and local permeability variations, up to around 3.5 mm from the block surface. The carbonation reaction produced a probable calcite-rich front with significantly reduced porosity that varied up to 50-100 µm in thickness. In contrast to the fill cement, the tail cement reacted extensively with the CO₂-rich synthetic marly porewater to produce a series of precipitates from a probable calcite and CSH gel, to ettringite and Ca-sulphate, chloride.

Although fluid chemical changes were not the main focus of this study, several observations were made that reflected water-cement-CO₂ reactions. In CO₂-free experiments the pH rose to about 12 as it equilibrated with the cement. However, in the presence of CO₂ this was brought down to about pH 7, and bicarbonate concentrations increased dramatically. Large decreases in Mg concentrations in the CO₂-free experiments suggest precipitation of a Mg-rich phase at high pH, whereas in the lower pH CO₂ experiments increases in Mg concentrations suggest dissolution. Data for Si show similar trends and suggest possible control by CSH phases. These types of changes are in general accord with known cement mineral behaviour.

In summary therefore, this relatively simple study into the reaction of CO₂ with borehole cements found no evidence for significant deleterious reactions – at least in the short term. However, our simple approach will have not replicated all of the complex spatial and temporal variations around a borehole. Much work remains to be done to develop a comprehensive understanding of the interactions of stored CO₂ with borehole cement, and especially those operating over the longer term.

References

- Bachu, S., Gunter, W.D. and Perkins, E.H. (1994). Aquifer disposal of CO₂: hydrodynamic and mineral trapping. *Energy Conversion and Management*, 35, 269-279.
- Bateman, K., Birchall, D.J., Rochelle, C.A., Pearce, J.M., Charlton, B.D., Reeder, S., Shaw, R.A., Taylor, H., Turner, G., and Wragg, J. (2004). Geochemical interactions between supercritical CO₂ and the Midale Formation. VI: Flow experiments with Midale Marly. British Geological Survey Commissioned Report, CR/04/010.
- Czernichowski-Lauriol, I., Sanjuan, B., Rochelle, C., Bateman, K., Pearce, J. and Blackwell, P. (1996). Area 5: Inorganic Geochemistry, Chapter 7 in 'The underground disposal of carbon dioxide' (S. Holloway ed.). Final report for the CEC, contract number JOU2-CT92-0031. Published by the British Geological Survey.
- DePuy, G.W., 1994. Chemical resistance of concrete. In: P. Klieger and J.F. Lamond (Editors) *Significance of Tests and Properties of Concrete and Concrete-Making Materials*, American Society for Testing and Materials, ASTM publication code number 04-169030-07, 263-281.
- Gibbs, W. W. 1996. Pressure to change, supercritical carbon dioxide to toughen common materials. *Scientific American*, November 1996, 27-28.
- Gunter, W.D., Perkins, E.H., Bachu, S., Law, D., Wiwchar, B., Zhou, Z. and McCann, T.J., 1993. Aquifer disposal of CO₂-rich gases. Alberta Research Council report, C-1993-5.
- Lee, F.M., 1970. *The chemistry of cement and concrete*, Edward Arnold, London.
- Mehta, P.K., 1994. Volume change. In: (P. Klieger and J.F. Lamond (Editors) *Significance of Tests and Properties of Concrete and Concrete-Making Materials*, American Society for Testing and Materials, ASTM publication code number 04-169030-07, 219-228.
- Moberg, R. (2001). *Greenhouse Issues* 57, 2.
- Reardon, E.J., James, B.R. and Abouchar, J., 1989. High pressure carbonation of cementitious grout. *Cement and Concrete Research*, 19, 385-399.
- Robins, N.S. and Milodowski, A.E., 1982. Design and evaluation of the Harwell borehole cement systems. Institute of Geological Sciences, Technical Report, ENPU 82-9.
- Rochelle, C.A., Bateman, K. and Pearce, J.M. (2002a). Geochemical interactions between supercritical CO₂ and the Utsira formation: an experimental study. British Geological Survey Commissioned Report, CR/02/060, 57 p.
- Rochelle, C.A., Birchall, D. and Bateman, K. (2002b). Geochemical interactions between supercritical CO₂ and the Midale Formation. I: Introduction to fluid-rock interaction experiments. British Geological Survey Commissioned Report, CR/02/289, 28 p.
- Rochelle, C.A., Birchall, D.J., Charlton, B.D., Reeder, S., Shaw, R.A., Taylor, H. and Wragg, J. (2002c). Geochemical interactions between supercritical CO₂ and the Midale Formation. II: Initial results of preliminary test experiments. British Geological Survey Commissioned Report, CR/02/290, 19 p.
- Rochelle, C.A., Birchall, D.J., Pearce, J.M., Charlton, B.D., Reeder, S., Shaw, R.A., Taylor, H., Turner, G., Wragg, J., Bateman, K. and McKervey, J.A. (2003a). Geochemical interactions between supercritical CO₂ and the Midale Formation.

III: Experiments investigating reactions of the Midale Marly. British Geological Survey Commissioned Report, CR/03/332, 34 p.

Rochelle, C.A., Birchall, D.J., Pearce, J.M., Charlton, B.D., Reeder, S., Shaw, R.A., Taylor, H., Turner, G., Bateman, K. and McKervey, J.A. (2003b). Geochemical interactions between supercritical CO₂ and the Midale Formation. IV: Experiments investigating reactions of the Midale Evaporite. British Geological Survey Commissioned Report, CR/03/333, 31 p.

Rochelle, C.A., Birchall, D.J., Pearce, J.M., Charlton, B.D., Reeder, S., Shaw, R.A., Taylor, H., Turner, G., Bateman, K. and McKervey, J.A. (2003c). Geochemical interactions between supercritical CO₂ and the Midale Formation. V: Experiments investigating reactions of the Midale Vuggy. British Geological Survey Commissioned Report, CR/03/334, 30 p.

Savage, D., Bateman, K., Hill, P., Hughes, C., Milodowski, A., Pearce, J., Rae, E. and Rochelle, C. (1992). Rate and mechanism of the reaction of silicates with cement pore fluids. *Applied Clay Science*, 7, 33-45.

Van Ginneken, L., Dutré, V., Adriansens, W. and Weyten, H. (2004). Effect of liquid and supercritical carbon dioxide treatments on the leaching performance of a cement-stabilised waste form. *Journal of Supercritical Fluids*, 30, 175-188.

Figure 1 Schematic diagram of the experimental arrangement used in this study.

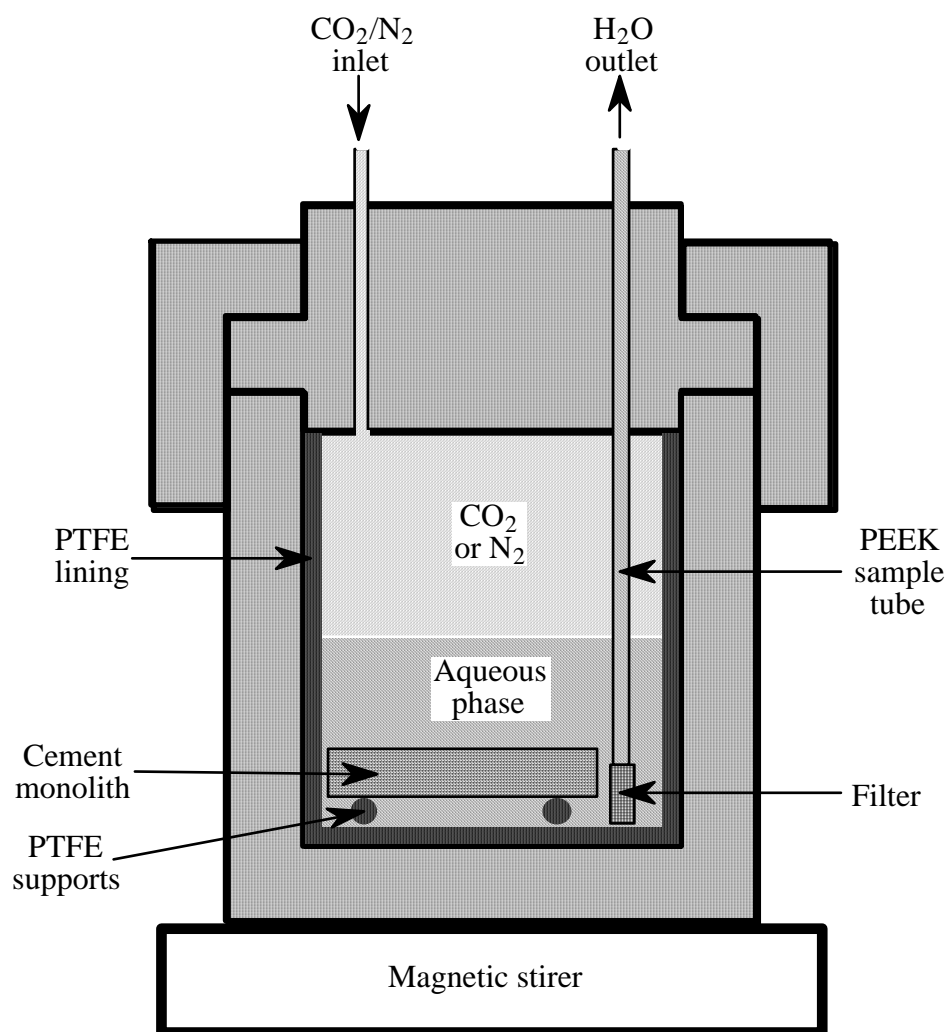


Figure 2 Schematic diagram of the Instron 3-point bend fixture.

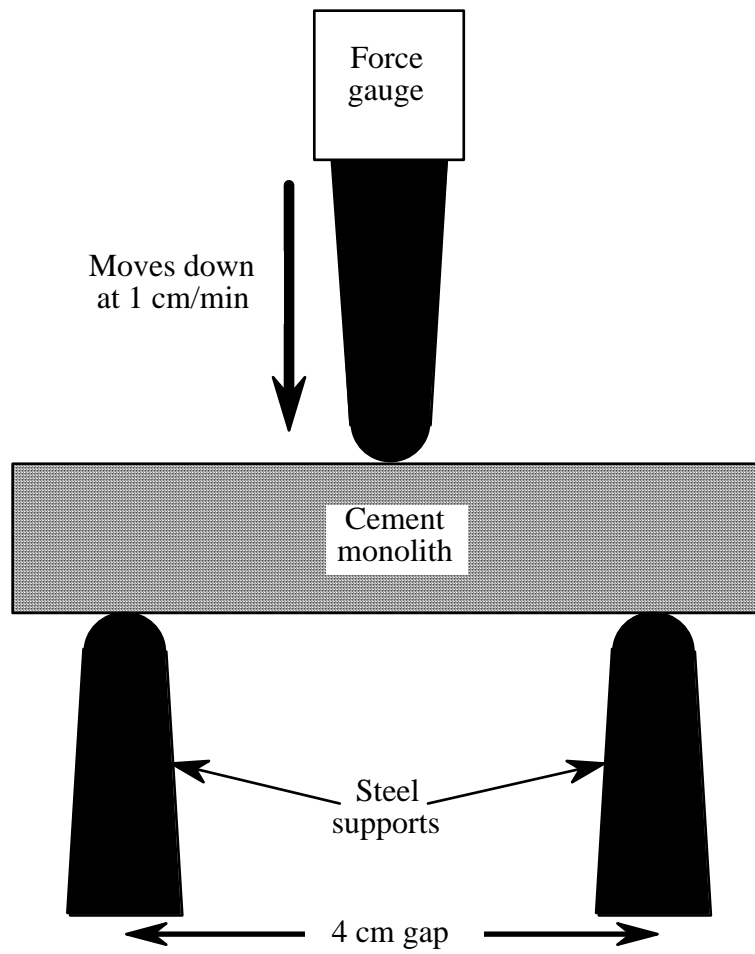
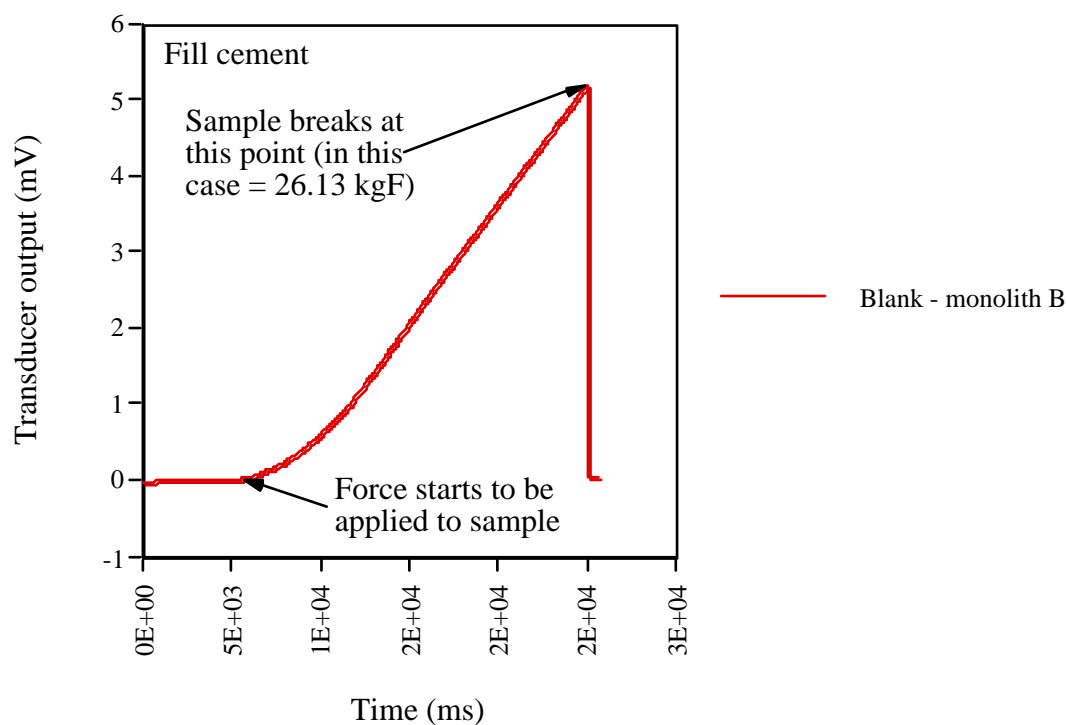
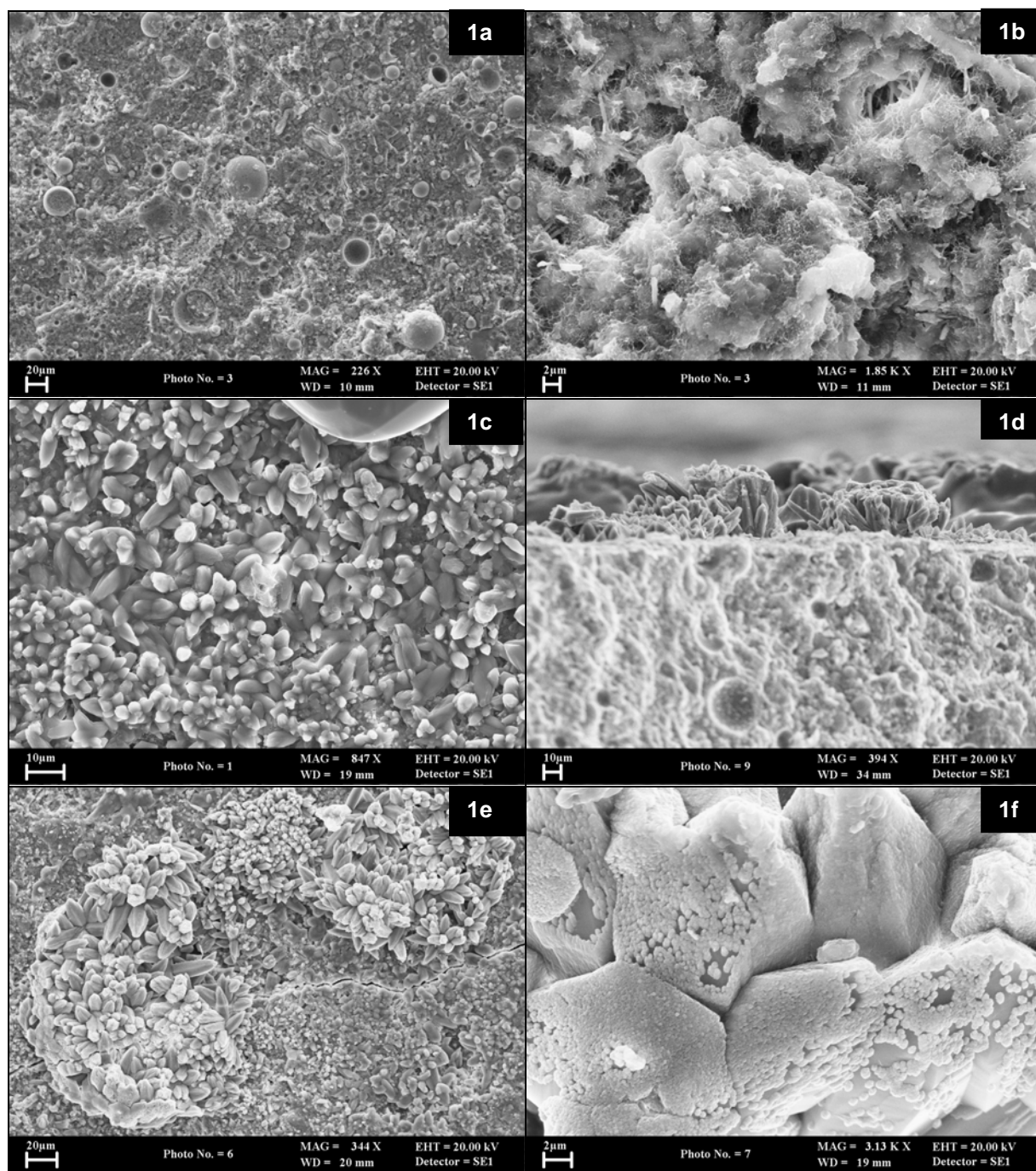
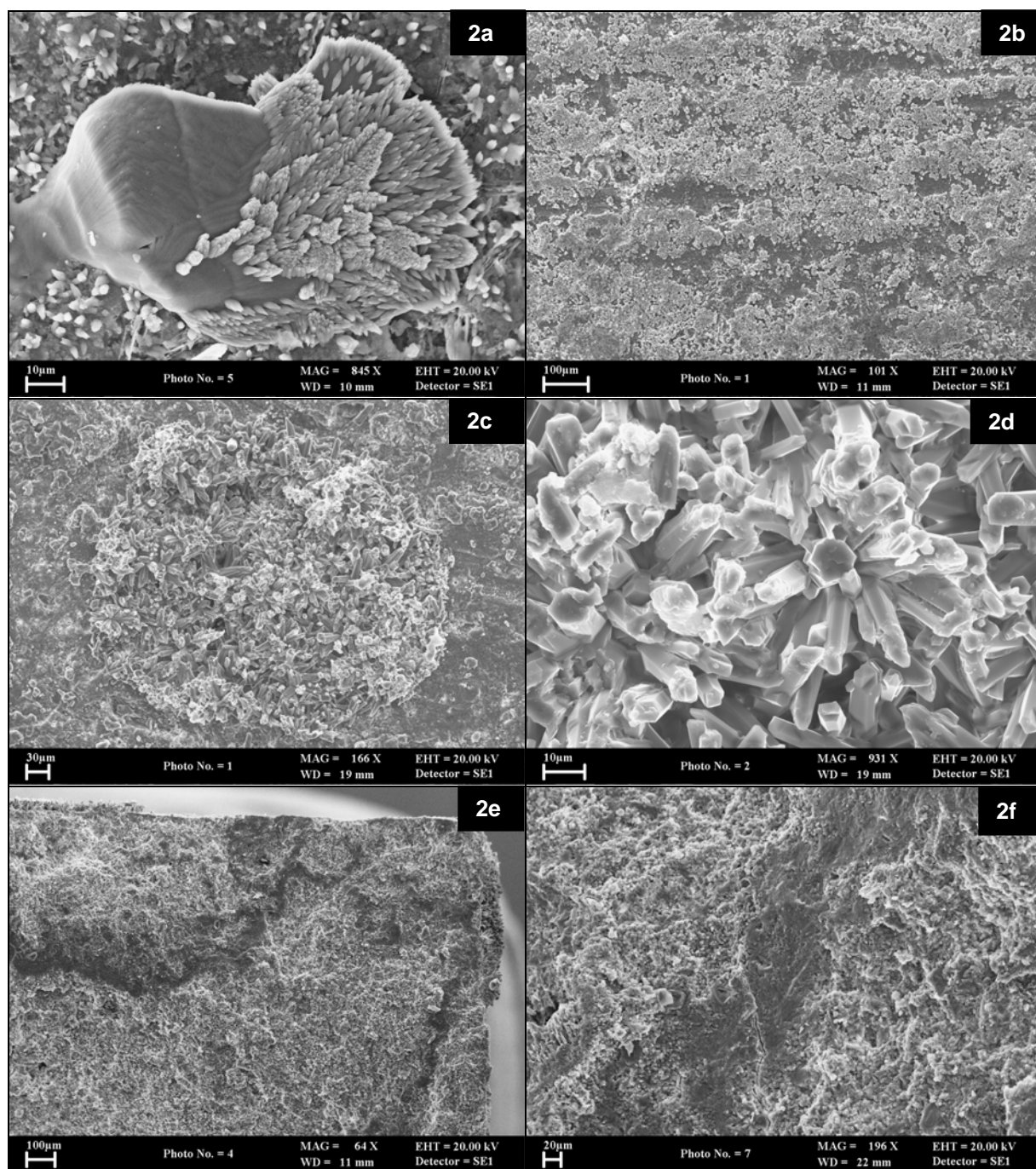


Figure 3 Diagrammatic representation of the output from the Instron tester during the testing of a typical cement monolith. Note that in this example, output voltage from the transducer is plotted rather than total force applied.

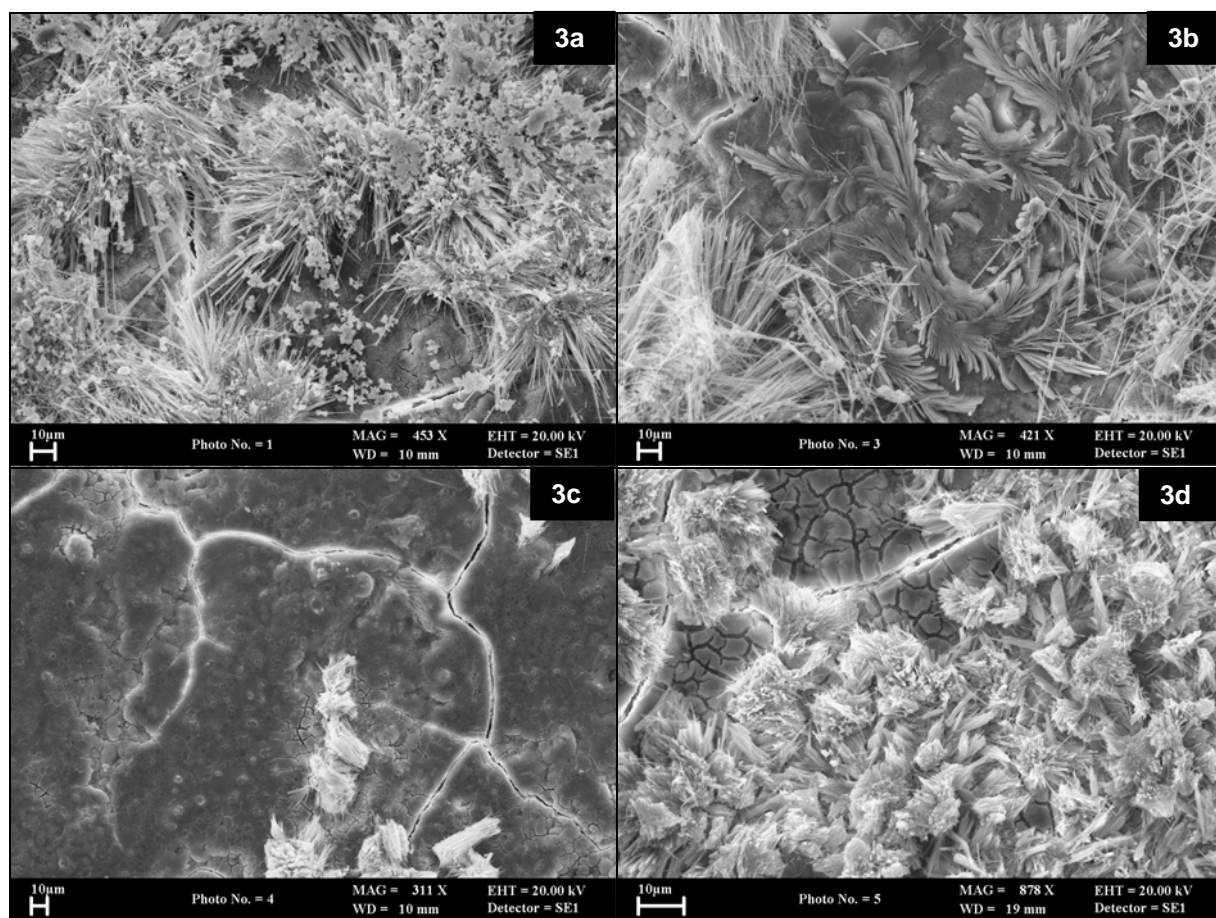




- Plate 1a Typical view of fine calcite coating external surface of the fill cement block (Run 1133, J980S101.tif).
- Plate 1b Tail cement matrix with a coalesced flaky texture and some fibrous outgrowths developed (Run 1135, J984S203.tif).
- Plate 1c Typical view of Fill cement block external surface (Run 1133, J981S203.tif).
- Plate 1d Oblique view of outer surface with calcite coating. (Run 1133, J980S201.tif).
- Plate 1e An example of clusters of radiating calcite crystals. Note that the crack cuts through the calcite crystals and may be an artefact of depressurisation (Run 1133, J980S106.tif).
- Plate 1f Detailed view of larger calcite crystals on the outer surface of the cement block, which are coated in fine-grained calcite (Run 1133, J980S107.tif).



- Plate 2a Detailed view of larger calcite crystals on the outer surface of the cement block, which are coated in fine-grained calcite (Run 1133, J981S105.tif).
- Plate 2b External surface of fill cement with patchy calcite coating (Run 1134, J982S101.tif).
- Plate 2c Typical aggregate clusters of calcite crystals coating external surface of tail cement block (Run 1135, J984S101.tif).
- Plate 2d Detailed view of calcite crystal morphologies (Run 1135, J984S102.tif).
- Plate 2e Tail cement matrix with clear alteration zone of denser, Ca-rich matrix, at variable depth. Note also patchy calcite precipitation on external block surfaces (Run 1135, J984S204.tif).
- Plate 2f Detail of internal tail cement block with dense alteration front (Run 1135, J985S204.tif).



- Plate 3a External surface of the tail cement block reacted with CO₂-charged synthetic marly porewater, coated in clusters of possible radiating ettringite (Run 1136, J986S101.tif).
- Plate 3b Curved hexagonal Ca,Al,chloride plates forming feather-like aggregates (Run 1136, J986S103.tif).
- Plate 3c Amorphous-looking homogenous, largely void-free, calcite and Ca,Al (±Cl) silicate hydrate layer coating that pre-dates other precipitates on external surface of the tail cement block reacted with CO₂-charged synthetic marly porewater (Run 1136, J986S104.tif).
- Plate 3d Irregular radiating ettringite aggregates post-dating amorphous-looking Ca sulphate,chloride coating.

Table 1 Listing of the CO₂ experiments conducted during this study, together with details of the sizes of the monoliths used.

Fill cement experiments										
Run no.	Monolith id.	Aqueous fluid	Gas	Measurement	Unreacted sample dimensions (mm)			Reacted sample dimensions (mm)		
					Height	Width	Length	Height	Width	Length
1133	A	None	CO2	1	10.85	11.67	48.63	10.99	11.65	48.88
"	"	"	"	2	10.32	11.72	-	10.60	12.16	-
"	"	"	"	3	10.51	11.98	-	10.51	12.32	-
1133	B	None	CO2	1	11.66	10.41	49.13	10.92	10.46	49.25
"	"	"	"	2	11.72	10.24	-	11.83	10.43	-
"	"	"	"	3	11.38	10.23	-	11.61	10.35	-
1134	C	SMFW	CO2	1	11.78	10.90	48.74	11.82	11.13	48.75
"	"	"	"	2	12.51	11.47	-	12.42	11.46	-
"	"	"	"	3	12.98	11.46	-	12.88	11.37	-
1134	D	SMFW	CO2	1	10.89	11.05	49.81	10.54	10.91	49.80
"	"	"	"	2	10.71	10.97	-	10.60	10.94	-
"	"	"	"	3	11.02	11.13	-	11.01	11.28	-
Tail cement experiments										
Run no.	Monolith id.	Aqueous fluid	Gas	Measurement	Unreacted sample dimensions (mm)			Reacted sample dimensions (mm)		
					Height	Width	Length	Height	Width	Length
1135	A	None	CO2	1	11.49	11.93	49.40	11.59	11.97	49.16
"	"	"	"	2	11.53	11.80	-	11.86	11.84	-
"	"	"	"	3	11.00	11.53	-	11.11	11.55	-
1135	B	None	CO2	1	11.27	11.56	49.36	11.34	11.56	49.36
"	"	"	"	2	11.34	11.23	-	11.34	11.28	-
"	"	"	"	3	11.24	10.76	-	11.28	10.95	-
1136	C	SMFW	CO2	1	11.82	11.04	51.66	11.74	10.86	51.71
"	"	"	"	2	11.82	11.22	-	11.90	11.17	-
"	"	"	"	3	11.43	11.23	-	11.60	11.17	-
1136	D	SMFW	CO2	1	11.85	11.00	51.58	11.82	10.92	51.63
"	"	"	"	2	11.41	11.71	-	11.45	11.61	-
"	"	"	"	3	10.98	11.73	-	10.89	11.81	-

SMFW = Synthetic Midale Marly formation water (based on analysis of a sample from well d8-23-6-14)

Table 2 Listing of all the experiments conducted during this study, together with details of the weights of the monoliths used.

Fill cement experiments						
Run no.	Monolith id.	Aqueous fluid	Gas	Initial wt (g)	Final wt (g)	% weight change
1133	A	None	CO ₂	11.2087	12.4896	11.4
	B	None	CO ₂	10.8648	12.0833	11.2
1134	C	SMFW	CO ₂	12.5718	13.8219	9.9
	D	SMFW	CO ₂	10.7483	11.7809	9.6
1139	A	SMFW	N ₂	14.2602	14.5075	1.7
	B	SMFW	N ₂	13.8041	13.9828	1.3
Tail cement experiments						
Run no.	Monolith id.	Aqueous fluid	Gas	Initial wt (g)	Final wt (g)	% increase in wt
1135	A	None	CO ₂	11.8120	12.2566	3.8
	B	None	CO ₂	11.1108	11.5731	4.2
1136	C	SMFW	CO ₂	11.9000	11.9747	0.6
	D	SMFW	CO ₂	12.0374	12.1395	0.8
1138	A	SMFW	N ₂	12.7395	12.7004	-0.3
	B	SMFW	N ₂	10.5771	10.5384	-0.4

SMFW = Synthetic Midale Marly formation water (based on analysis of a sample from from well d8-23-6-14)

Table 3 Listing of all the experiments conducted during this study, together with details of the strengths of the monoliths tested.

Fill cement experiments					
Run no.	Monolith id.	Aqueous fluid	Gas	Instrom strength tester output kgF	Instrom strength tester output V
Blank	A	-	-	34.31	6.830
	B	-	-	26.13	5.195
1133	A	None	CO2	33.76	6.730
	B	None	CO2	34.30	6.834
1134	C	SMFW	CO2	39.42	7.860
	D	SMFW	CO2	32.15	6.404
1139	A	SMFW	N2	17.91	(3.563)
	B	SMFW	N2	20.55	4.088
Tail cement experiments					
Run no.	Monolith id.	Aqueous fluid	Gas	Instrom strength tester output kgF	Instrom strength tester output V
Blank	A	-	-	20.21	4.029
	B	-	-	14.46	2.876
1135	A	None	CO2	13.15	2.608
	B	None	CO2	14.27	2.833
1136	C	SMFW	CO2	7.637	1.512
	D	SMFW	CO2	(7.180)	1.421
1138	A	SMFW	N2	n/d	n/d
	B	SMFW	N2	16.53	3.294

SMFW = Synthetic Midale Marly formation water (based on analysis of a sample from well d8-23-6-14)
n/d = no data due to logger failing

Appendix 1

Formatted analytical data for aqueous fluids from the borehole experiments that are described in this report.